

ORIGINAL ARTICLE

Biomanufacturing of Axon-Based Tissue Engineered Nerve Grafts Using Porcine GalSafe Neurons

Kritika S. Katiyar, PhD,¹⁻³ Justin C. Burrell, PhD,^{2,3} Franco A. Laimo, BS,^{2,3} Kevin D. Browne, BA,^{2,3} John R. Bianchi, PhD,⁴ Anneke Walters, PhD,⁴ David L. Ayares, PhD,⁴ Douglas H. Smith, MD,^{1,2} Zarina S. Ali, MD,^{2,3} Harry C. Ledebur, PhD,^{1,5} and D. Kacy Cullen, PhD¹⁻³

Existing strategies for repair of major peripheral nerve injury (PNI) are inefficient at promoting axon regeneration and functional recovery and are generally ineffective for nerve lesions >5 cm. To address this need, we have previously developed tissue engineered nerve grafts (TENGs) through the process of axon stretch growth. TENGs consist of living, centimeter-scale, aligned axon tracts that accelerate axon regeneration at rates equivalent to the gold standard autograft in small and large animal models of PNI, by providing a newfound mechanism-of-action referred to as axon-facilitated axon regeneration (AFAR). To enable clinical-grade biomanufacturing of TENGs, a suitable cell source that is hypoimmunogenic, exhibits low batch-to-batch variability, and able to tolerate axon stretch growth must be utilized. To fulfill these requirements, a genetically engineered, FDA-approved, xenogeneic cell source, GalSafe[®] neurons, produced by Revivicor, Inc., have been selected to advance TENG biofabrication for eventual clinical use. To this end, sensory and motor neurons were harvested from genetically engineered GalSafe day 40 swine embryos, cultured in custom mechanobioreactors, and axon tracts were successfully stretch-grown to 5 cm within 25 days. Importantly, both sensory and motor GalSafe neurons were observed to tolerate established axon stretch growth regimes of ≥ 1 mm/day to produce continuous, healthy axon tracts spanning 1, 3, or 5 cm. Once stretch-grown, 1 cm GalSafe TENGs were transplanted into a 1 cm lesion in the sciatic nerve of athymic rats. Regeneration was assessed through histological measures at the terminal time point of 2 and 8 weeks. Neurons from GalSafe TENGs survived and elicited AFAR as observed when using wild-type TENGs. At 8 weeks postrepair, myelinated regenerated axons were observed in the nerve section distal to the injury site, confirming axon regeneration across the lesion. These experiments are the first to demonstrate successful harvest and axon stretch growth of GalSafe neurons for use as starting biomass for bioengineered nerve grafts as well as initial safety and efficacy in an established preclinical model—important steps for the advancement of clinical-grade TENGs for future regulatory testing and eventual clinical trials.

Keywords: neural tissue engineering, biomanufacturing, axon regeneration, tissue engineered medical product, tissue engineered nerve graft

Impact Statement

Biofabrication of tissue engineered medical products requires several steps, one of which is choosing a suitable starting biomass. To this end, we have shown that the clinical-grade, genetically engineered biomass—GalSafe[®] neurons—is a viable option for biomanufacturing of our tissue engineered nerve grafts (TENGs) to promote regeneration following major peripheral nerve injury. Importantly, this is a first step in clinical-grade TENG biofabrication, proving that GalSafe TENGs recapitulate the mechanism of axon-facilitated axon regeneration seen previously with research-grade TENGs.

¹Axonova Medical, LLC, Philadelphia, Pennsylvania, USA.

²Center for Brain Injury & Repair, Department of Neurosurgery, Perelman School of Medicine, University of Pennsylvania, Philadelphia, Pennsylvania, USA.

³Center for Neurotrauma, Neurodegeneration & Restoration, Corporal Michael J. Crescenz Veterans Affairs Medical Center, Philadelphia, Pennsylvania, USA.

⁴Revivicor, Inc., Blacksburg, Virginia, USA.

⁵Battelle Memorial Institute, Columbus, Ohio, USA.

Introduction

TISSUE ENGINEERED MEDICAL products (TEMPs) hold tremendous promise as regenerative therapies to transform the treatment of a myriad of disorders and diseases. Biomanufacturing of TEMPs for clinical use involves transitioning from a laboratory-based process of essentially prototype development to a process encompassing current good manufacturing practices (cGMP) to enable reproducible fabrication of safe and potent product. This transition to a cGMP process involves several critical steps, including choosing suitable (i.e., cGMP-compliant and effective) starting biomass and materials; growth, maturation, and survival within an appropriate bioreactor; establishment of quality assurance (QA) and release criteria; and storage and transport of the product to the clinic for use in patients.

As one of the most important initial steps, choosing the appropriate starting biomass may pose several challenges as individual specifications must be taken into consideration to serve each unique application. For example, when potential lack of availability and/or high costs prevent the use of autologous cells, the need for immune suppression generally must be considered to avoid a detrimental host response to the TEMP. While the use of human stem cell-derived mature cells may partially mitigate an immune response (e.g., if HLA matching is performed), the use of allogeneic human stem cells present challenges for clinical-grade manufacturing, including batch-to-batch variability in differentiation; a requirement of considerable time (i.e., weeks to months) and agents (e.g., genetic modifiers, growth factors) for differentiation, which add to the cost-of-goods; and the potentially devastating effects of de-differentiated or non-differentiated cells becoming tumorigenic. These various considerations and trade-offs in biomanufacturing and performance apply broadly to TEMPs for treatment of virtually any organ system, including the nervous system, and therefore should be carefully considered as the selection of an appropriate starting biomass provides the foundation upon which the remainder of cGMP process is built.

In certain cases, an attractive source for the starting biomass for TEMP biofabrication would be from xenogeneic sources, which are readily accessible, provide fully differentiated cells—without time-consuming, expensive, and inconsistent differentiation protocols—and are unlikely to contain tumorigenic cells. Here, porcine tissue and/or cells have gained particular interest due to size, genetic, and functional similarities with humans.^{1–4} However, to date, xenotransplantation products (tissues with viable cells) from pigs have seen limited acceptance, apart from glutaraldehyde-fixed heart valves, as sources for clinical transplantation mainly due to rapid immune rejection.^{5–8} Apart from measures to ensure acceptance of the xenogeneic product by the host, FDA guidelines for cGMP of xenogeneic products, similarly to cGMP guidelines for nonxenogeneic products, state that precautions should be taken to avoid contamination/cross-contamination of the product as well as validation of supplies and surroundings such as air, water, and equipment used during manufacturing of the product.⁹

Very few xenogeneic tissue engineered cell based products exist in the market, with no known products for neural regeneration. However, products such as Diabecell[®] (Diatranz Otsuka Ltd.), which are microencapsulated pig

islet cells for the treatment of diabetes, reported processes to ensure microbial safety of source animals and safety and efficacy in nonhuman primate models.^{10–13} For autologous products (MACI or Carticel, Vericel), the main focus was on viability, sterility, growth, morphology, and reproducibility, along with safety and efficacy studies.¹⁴ For allogeneic products such as Apligraf[™] by Organogenesis, preclinical studies also included characterization of the cells and final product as well as immunology studies (effect on T cell proliferation, MHC class II molecules, etc.).¹⁵

The tissue incompatibility for xenogeneic cells is primarily driven by the ubiquitous presence of the endogenous antigen, galactose- α 1,3-galactose (gal).^{16,17} While other antigens do exist, these can be mitigated with the use of common immunosuppressants. In contrast, gal expression is more widespread, as ~1% of all immunoglobulins in humans are anti-gal antibodies, and can elicit a vigorous acute immune response.¹⁷ Gal expression results from the catalytic activity of the α 1,3-galactosyltransferase enzyme encoded by the glycoprotein α 1,3-galactosyltransferase gene (GGTA1).^{18–21} Certain mammalian species, such as catarrhines (humans, apes, and Old World monkeys), do not have a functional GGTA1 gene and correspondingly do not express gal.^{20,22,23} In addition, gal has been documented to be absent in plants, fish, amphibians, reptiles, and birds.^{20,24,25} The function of gal is unknown, but is clearly not essential for survival.^{20,26} Indeed, gal is the major antigen on pig cells/tissues to which human anti-gal antibodies bind.²⁷ Thus, following pig cell, tissue, or organ transplant into catarrhines, anti-gal antibodies readily bind to gal and thereby activate the complement system within minutes to hours, resulting in rapid graft rejection.^{7,8,27} To overcome this challenge, Revivicor, Inc. has utilized its expertise in somatic cell nuclear transfer (SCNT) in combination with gene targeting techniques to establish a unique proprietary genetically engineered pig line that has no detectable gal present.^{19,28–30}

This technology and subsequent breeding has resulted in the development of a line of pigs referred to as GalSafe[®]. GalSafe pigs are intended to provide a source of raw materials for fabrication and distribution as implantable medical products for human use. Xenogeneic GalSafe tissue may primarily act as a temporary scaffold that retains many endogenous factors to promote healing and/or recellularization with host cells during the regenerative process, and then ultimately can be resorbed by the body. In addition, GalSafe tissue grafts are commonly regarded as immunogenically quiescent due to the lack of gal expression. Thus, the use of a genetically modified xenogeneic cell source that is hypo-immunogenic, readily available, and provides fully differentiated cells, obviating the need for long differentiation times, and absent concerns of de-differentiation into tumorigenic cells, may provide a promising solution to many cell source challenges in TEMP biomanufacturing and efficacy.

One area where an effective TEMP would hold particular promise is in repair of segmental defects (i.e., gaps) in peripheral nerves, a common occurrence due to vehicular accidents, assaults, trauma to combat personnel, and as a result of surgery (e.g., tumor resection), among other causes.³¹ While peripheral nerves possess an innate ability to regenerate, it is generally a slow and inefficient process,

often leaving patients afflicted with major peripheral nerve injury (PNI) with permanent disabilities. Indeed, ~20 million Americans alone suffer from residual effects of PNI, resulting in \$50 billion in health care costs annually.³⁰ Clinically, biomaterial-based nerve guidance tubes (NGTs) and acellular nerve allografts (ANAs) are most commonly used to repair nerve lesions up to 2 cm; however, due to the lack of living cues, they remain largely ineffective for larger nerve gaps. Major PNIs are particularly challenging as these injuries exhibit a large nerve gap (≥ 3 cm) and/or proximal nerve injury, which inherently necessitate long distances for host axons to regrow to successfully reinnervate distal end targets (e.g., skin, muscle). In these cases, the autologous nerve graft (autograft) remains the gold standard to repair major nerve lesions.³³ However, the use of autografts requires deliberately creating a deficit to take otherwise healthy nerve to surgically repair a damaged nerve. Because of this and the potential unavailability of healthy autologous donor nerve, the use of allografts has also been implemented; although the use of allografts may pose serious immunogenicity risks and generally require immune suppression. Despite this range of treatment options, none is consistently satisfactory as only ~50% of repaired nerves achieve meaningful functional recovery regardless of the treatment option.^{33,34}

To address this need, our research group has developed tissue engineered nerve grafts (TENGs) as the first “living scaffolds” specifically designed to recapitulate developmental mechanisms of axon regeneration while maintaining the efficacy of proregenerative guidance pathways and muscle receptiveness to reinnervation. This results in accelerated axon regeneration, more robust muscle reinnervation, as well as promoting the health of spinal motor neurons, all of which effectively increase attainable levels of functional recovery.^{35–37} TENGs consist of long (e.g., centimeter-scale), aligned, living axon tracts fabricated through the process of axon stretch growth within custom mechanobioreactors.^{36–39}

Our process of axon stretch growth mimics the process seen during development. During early embryogenesis, axons form connections with end targets and are “stretch-grown” as the body grows through adulthood. We have successfully recapitulated this process to rapidly produce long axon tracts spanning up to 5 cm in <21 days. To date, axon stretch growth has been demonstrated from numerous neuronal subtypes and species, including rodent embryonic sensory, motor, and cortical neurons^{36,38–40}; porcine embryonic sensory and motor neurons; and human adult sensory neurons and induced pluripotent stem cells (iPSC)-derived cortical neurons.^{41,42} Upon transplantation of allogeneic TENGs to bridge segmental defects in rat and porcine models of PNI, regenerating host axons were seen to grow directly along transplanted TENG axons,^{36–38} a phenomenon referred to as axon-facilitated axon regeneration (AFAR) that is believed to be a key mechanism by which TENGs promote functional recovery.³⁷ Along with evidence of AFAR, preclinical studies in our small and large animal PNI models confirmed that TENGs promoted functional recovery at least equivalent to autografts and performed far superior to NGTs alone.³⁷ Our group has previously fabricated sensory-only and mixed motor-sensory TENGs to promote regeneration of sensory nerves and mixed and/or motor nerves, respectively.³⁸

The objective of the current study is to advance TENG biomanufacturing by using neurons derived from GalSafe pigs as the starting biomass. Of note, the current study is an academic-industry collaboration intended to facilitate the translation of TENG biomanufacturing from a laboratory-based to a clinical-grade process in conjunction with Axonova Medical, LLC (the commercializing entity for TENGs and other nerve-related TEMPs) and Revivicor, Inc. (provider of GalSafe porcine tissue), who has recently gained FDA approval for their GalSafe pigs as a suitable source for human use. Here, we report the successful biofabrication of TENGs featuring stretch-grown axon tracts from genetically modified embryonic neurons from GalSafe pigs. We also demonstrate that these novel GalSafe TENGs are effective in an athymic rat model of segmental nerve defects, showing graft neuron survival, recapitulation of AFAR, and dense host axonal regeneration across the repair zone. Moving forward, these promising results will enable a full transition to a cGMP-compliant process for TENG biofabrication to facilitate investigational new drug (IND)-enabling preclinical studies to evaluate the safety, tolerability, and efficacy of GalSafe TENGs before clinical trials.

Methods

All procedures were approved by the Institutional Animal Care and Use Committees at the University of Pennsylvania and Michael J. Crescenzo Veterans Affairs Medical Center and adhered to the guidelines set forth in the NIH Public Health Service Policy on Humane Care and Use of Laboratory Animals (2015). Fetus collection occurred under protocols approved by the Institutional Animal Care and Use Committees at Revivicor, Inc.

Biofabrication of TENGs

The process to biofabricate GalSafe TENGs is described in Figure 1.

Fabrication of sensory GalSafe constructs. Embryonic day 40 (E40) GalSafe porcine embryos were collected from a pregnant GalSafe sow and shipped on ice overnight from Revivicor, Inc., containing a mix of wild-type (WT), single-knockout (SKO), and double-knockout (DKO) embryos. Each embryo was packaged individually and labeled to separate the different phenotypes. Immediately upon arrival, the spinal cord was extracted and whole dorsal root ganglia (DRG) were harvested and cultured in Neurobasal[®] medium supplemented with 2% B-27, 500 μ M L-glutamine, 1% fetal bovine serum (Atlanta Biologicals), 2.5 mg/mL glucose (Sigma), 10 ng/mL 2.5S nerve growth factor (BD Biosciences), 10 μ M 5FdU (Sigma), 20 μ M uridine (Sigma), and 0.1% penicillin/streptomycin.

Explants were plated either in standard polystyrene tissue culture-treated well plates coated with 40 μ g/mL poly-D-lysine (PDL; BD Biosciences) and 40 μ g/mL laminin (BD Biosciences) or within custom-built mechanobioreactors designed for “stretch growth” of integrated axonal tracts. These chambers contained two membranes of 33C Aclar (SPI supplies) treated with 40 μ g/mL PDL and 40 μ g/mL laminin. One of these membranes, denoted the “towing membrane,” could be precisely moved by a stepper motor, while the other, denoted the “base membrane,” remained

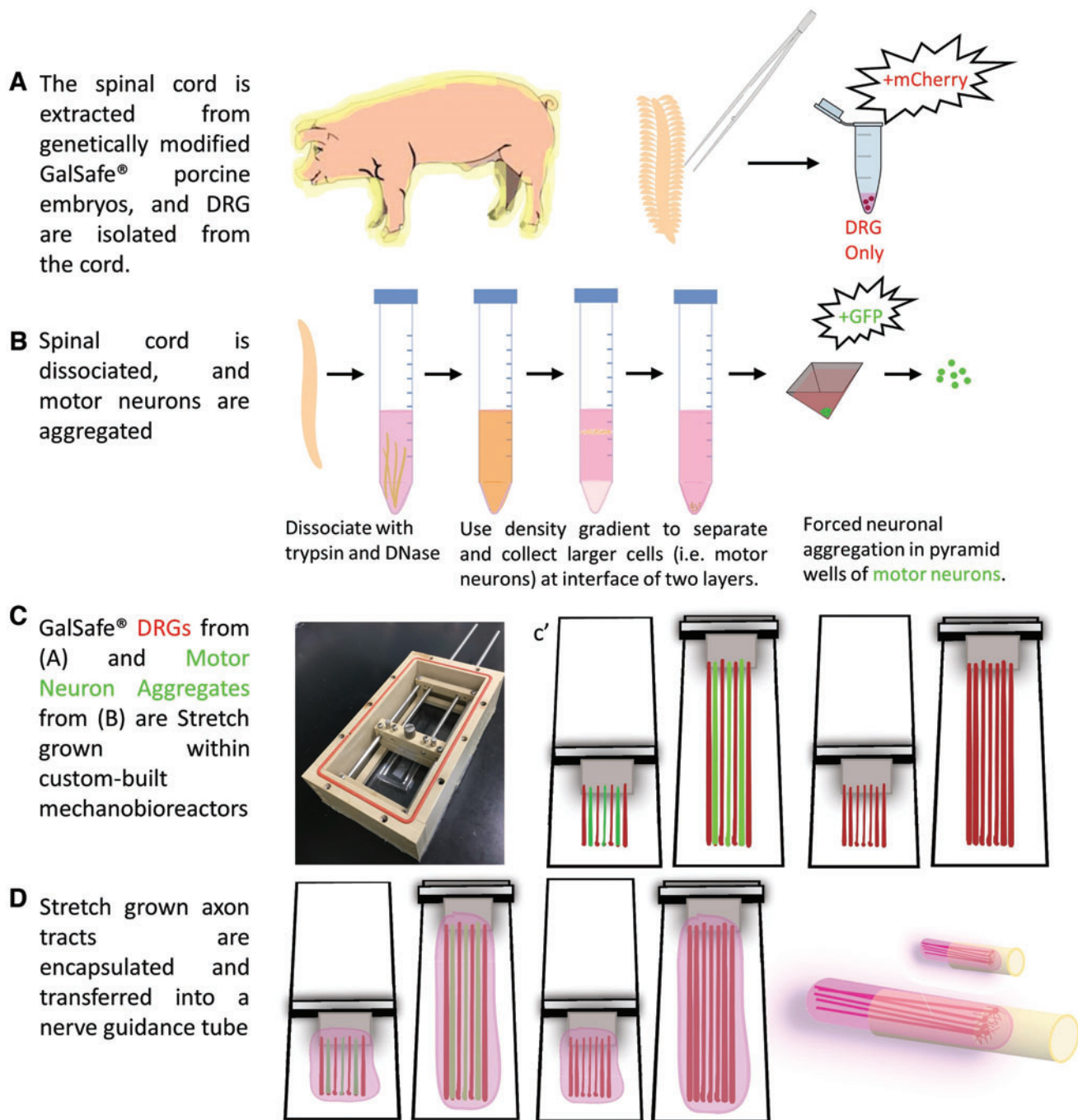


FIG. 1. Biomanufacturing of GalSafe® TENGs. **(A)** Spinal cord is harvested from an embryonic day 40 (E40) GalSafe swine fetus, and the sensory DRG are plucked and stored in L-15 medium. **(B)** After the cord is stripped of DRG and any remaining connective tissue, it is dissociated using 2.5% Trypsin+EDTA and DNase and motor neurons are collected using a density gradient. A single-cell suspension of motor neurons is then added to an inverted pyramid well to form aggregates. The DRG and/or motor neuron aggregates are then plated within the custom built mechanobioreactor, and axons are subsequently stretch-grown to either 1, 3, or 5 cm. **(C)** Image of actual bioreactor and (c') schematic representation of mixed motor-sensory neurons (*green*—motor neuron aggregates; *red*—sensory DRG) or sensory only neurons (*red*), each with axon tracts stretch-grown to 1 cm or 5 cm in length. **(D)** Once the axon tracts have reached the desired length, they are encapsulated in a collagenous matrix and transferred to an appropriately sized commercially available NGT. For manufacturing, quality control and cGMP measures of GalSafe pigs, such as testing for infectious agents, animal welfare, animal and herd qualification, and harvest and shipping of GalSafe embryos are implemented. For TENG manufacturing, quality control and cGMP measures will be put in place control for sensory and/or motor neuron number and aggregate size, stretch-grown axon length, and health. cGMP, current good manufacturing practices; DRG, dorsal root ganglia; NGT, nerve guidance tube; TENGs, tissue engineered nerve grafts. Color images are available online.

fixed. The DRGs were plated in two populations on either side of the membrane interface.³⁸ In particular, the towing membrane was 1 cm wide, with 20 DRG plated in total (with 10 DRG on the base membrane and 10 DRG on the towing membrane) when used to make 1 cm long stretch-grown constructs. When stretching axons to 3 or 5 cm, the cell and axon density was increased and therefore the towing membrane was 2 cm wide with a total of 40 DRG (with 20 DRG on the base membrane and 20 DRG on the towing membrane). Axonal networks were allowed to form between the two DRG populations at the membrane interface for 5 days *in vitro* (DIV) before applying displacement and therefore initiating "stretch growth." At 4 DIV, GFP-AAV vector was added to the media for 24 h to allow for GFP transduction of the cells. The next day, a full media change was done, and the stepper motor system was engaged to gradually, but continuously, separate the populations in micron-size increments until the TENGs reached their desired lengths. To stretch grow axons 1 cm, the rate of displacement was kept constant at 1 mm/day for 2 days, then 2 mm/day for 4 days. To stretch grow axons 3 cm, displacement began at 1 mm/day for 1 day, followed by 2 mm/day for 2 days, and finally 3 mm/day for 9 days. Likewise, to stretch grow axons to 5 cm, the rate of displacement was initially 1 mm/day for 1 day, and it was then increased to 2 mm/day for 2 days, followed by 3 mm/day for 15 days until the desired length of 5 cm was obtained. A half media change was completed once every week.

Fabrication of mixed GalSafe constructs. Once all DRG were removed from the spinal cord, the cord was dissociated using trypsin and DNase.^{38,43} A single-cell solution of motor neurons was obtained via a density gradient using bovine serum albumin and OptiPrep®. The single-cell solution was either plated in tissue culture-treated well plates coated with PDL and laminin at a density of 8×10^4 cells or added to inverted pyramid wells and centrifuged at 2000 RPM for 5 min to form an aggregate of motor neurons.^{38,44,45} After allowing the aggregates to stabilize within the inverted pyramid wells, the aggregates were extracted and individually plated either within well plates coated with PDL and laminin as described above or the mechanobioreactors (treated with PDL and laminin). In the case of the latter, we alternated sensory DRG and motor neuron aggregates totaling 20 cell clusters (with 5 DRG and 5 motor neuron aggregates on the towing membrane and base membrane each) for 1 cm stretch growth. For 3 and 5 cm stretch growth, alternating sensory DRG and motor neuron aggregates totaling 40 cell clusters (with 10 DRG and 10 motor neuron aggregates on the towing membrane and base membrane each) were placed along the interface of the towing membrane.

Motor neurons were cultured in glial conditioned media supplemented with 37 ng/mL hydrocortisone, 2.2 µg/mL isobutylmethylxanthine, 10 ng/mL brain-derived neurotrophic factor (BDNF), 10 ng/mL ciliary neurotrophic factor (CNTF), 10 ng/mL cardiotropin-1 (CT-1), 10 ng/mL glial-derived neurotrophic factor (GDNF), 2% B-27, 20 ng/mL NGF, 20 µM mitotic inhibitors, 2 mM L-glutamine, 417 ng/mL forskolin, 1 mM sodium pyruvate, 0.1 mM β-mercaptoethanol, and 2.5 g/L glucose, as previously described.^{38,43} To stretch grow the mixed motor-sensory axons, axon net-

works were allowed to form before applying displacement. Similarly to sensory-only constructs, GFP-AAV vector was added to the media to transduce DRG and motor neuron aggregates for 24 h. The next day, a full media change was done and axon stretch growth was initiated. To initiate axon stretch growth to 1 cm, constant displacement at a rate of 1 mm/day for 10 days was applied.

Encapsulation of stretch-grown constructs. Once the terminal length was reached, the health of TENGs was measured on a semiquantitative score that accounted for the health of the axons as determined by the amount of proteinaceous build up observed along the length of the axon tracts and density of continuous and intact axons within the tracts. A score of 1–5 was given based on these criteria, with a score of 1 having very few, if any intact axon tracts and/or extreme protein build up along axons leading to discontinuous axons; and a score of 5 being the most healthy TENG with dense, continuous axons exhibiting minimal to no protein build up (Table 1). Only TENGs with a health score of 4 or 5 were transplanted. Stretch-grown cultures were encapsulated in an extracellular matrix (ECM) composed of rat-tail collagen type I (BD Biosciences) supplemented with 2.5S nerve growth factor (BD Biosciences). After gelation at 37°C, embedded cultures were manipulated into cylinders, removed from the membranes, and placed within a nerve guidance conduit (Stryker NeuroFlex™ Nerve Guidance).

Peripheral nerve surgery and repair

Experimental subjects were adult male rats (RNU Athymic, Charles River). Rats were anesthetized with inhaled isoflurane (5% induction and 2.5% maintenance). The left rat sciatic nerve was exposed and a 1.0 cm segment was excised and replaced with an autologous nerve graft (1.0 cm long only; reversal of excised nerve; $n=4$), an NGT (1.0 cm long only; filled with the same ECM+NGF used to encapsulate TENGs; $n=4$), or a TENG within an NGT (1.0 cm; $n=9$). Constructs were implanted by inserting the two nerve stumps into the ends of the NGT, which were sutured to the epineurium using four 8–0 absorbable sutures. The wound site was closed with 4–0 prolene or nylon sutures.

Nerve harvest and histology

GalSafe nerve. Unmodified (control) and GalSafe pigs (test samples) were euthanized under IACUC approved

TABLE 1. AXON HEALTH SCORE (ONLY SCORES ≥ 4 CONSIDERED FOR TRANSPLANTATION)

Score	Description
1	Individual axons with obvious beading and degeneration. Less than 10% axon density.
2	Individual axons, irregular surface or beading along length. Less than 25% axon density.
3	Small fascicles or individual axons, some surface irregularities. Less than 50% axon density.
4	Dense axons, smaller, fascicles, regular/smooth structure. Up to 75% axon density.
5	Dense, thick, homogenous axon fascicles. Greater than 75% axon density.

protocols. Samples of the intercostal nerves were collected along the rib cage within 30 min after death and preserved into 10% NBF (Neutral Buffered Formalin). Small sections (<4 mm) were cut from both control and test samples and embedded in paraffin wax blocks following a standard protocol for tissue processing. 4–5 μ m sections were cut from the paraffin blocks, transferred to slides, deparaffinized, hydrated, and subsequently stained with GSL I-B4 (biotinylated Griffonia Simplicifolia Lectin, isolectin B4; Cat. No. B-1205; Vector Laboratories). Following the lectin staining step, the slides were counter stained with hematoxylin. The presence or absence of α -Gal were determined by the staining results, a brown colored conjugate was indicative of a positive results, while a light blue color and the absence of brown staining was associated with a negative result, thus absence of α -Gal.

Repaired rat nerve. At time of harvest, rats were overdosed with sodium pentobarbital. The entire length of the repaired nerves was harvested and placed in 4% paraformaldehyde for 48 h at 4°C. The excised tissue was immersed in 30% sucrose solution for 48 h or until fully saturated. For acute (2 weeks) animals, the entire repair zone and distal nerve segments were cryosectioned longitudinally (20–25 μ m thickness) and for chronic (8 weeks) animals, nerve cross-sections were cryosectioned axially (10 μ m thickness), mounted on glass slides, and immunolabeled. Longitudinal and/or axial sections were labeled using the following primary antibodies (1) mouse SMI31/32 (neurofilament, 1:1500 frozen; Millipore), (2) rabbit S-100 (1:250; Invitrogen), and/or (3) rabbit myelin basic protein (MBP, 1:500; Sigma). Secondary fluorophore-conjugated antibodies (AlexaFluor—568, and/or 647; or Jackson ImmunoResearch) were used as appropriate.

Imaging, quantification, and statistical analyses

Immunocytochemistry of neuronal cultures. Nonstretch-grown cultures were fixed with 4% formalin for 30 min at 9 DIV and stretch-grown TENGs were fixed at 11 DIV after reaching 1 cm and being encapsulated in the collagen matrix described above. After fixation, the cultures were blocked with normal horse serum for 60 min, and incubated overnight in mouse β -tubulin (Tuj1; 1:500; Abcam), sheep choline acetyl transferase (ChAT; 1:500; Abcam), rabbit glial fibrillary acidic protein (GFAP; 1:500; Millipore). The following day, secondary fluorophore-conjugated antibodies (AlexaFluor—568, and/or 647; or Jackson ImmunoResearch) were used as appropriate along with HOECHST nuclear stain.

Microscopy. Stretch-grown constructs were imaged under phase contrast and fluorescent microscopy by Nikon Eclipse Ti-S with digital image acquisition using a QiClick camera interfaced with Nikon Elements Basic Research software (4.10.01). The sections were examined under an epifluorescent microscope (Eclipse E600; Nikon, Melville, NY), and the images were digitally captured (Spot RT Color; Diagnostic Instruments, Sterling Heights, MI). Alternatively, the *in vivo* sections were fluorescently imaged using a laser scanning confocal microscope (AR1; Nikon).⁴⁶

Axon characterization. Axon characterization and *in vitro* TENG health scores were scored by a blinded researcher.

Nonstretch-grown cultures. Phase/contrast images of cultures *in vitro* up to 14 days were acquired. The axon length radially from the cell body region was measured in eight equidistant locations around individual sensory DRG or motor neuron aggregates, and averaged resulting in the axon outgrowth for that cluster. The effect of culture type (dissociated motor neurons vs. aggregated motor neurons, and DRG) on axon length was compared over time using a two-way analysis of variance (ANOVA). The ANOVA showed that there was a large effect associated with time and culture type based on $F(6, 16) = 134.8, p < 0.0001$.

Stretch-grown cultures. Axon coverage measures the amount of the towing membrane length that is covered in axons (the towing membrane is 1 cm long for axons stretch-grown to 1 and 2 cm long for axons stretch-grown to 3 and 5 cm). This measure relates to the axon density, and is indicative of cell and, subsequently, TENG health. Once stretch-grown, the area of axon coverage was measured using Fiji software for WT, SKO, and DKO constructs spanning 1, 3, and/or 5 cm by overlaying a grid, and measuring the length of areas within one construct lacking axon or fascicle outgrowth equidistant from the edge of the cell body region were measured and summed.³⁸ TENG axon characterization was analyzed using one-way ANOVA to determine the effect of TENG length on TENG health, axon density, and fascicle diameter. All quantification except for 1 cm axon density passed the test of equal variance (Brown-Forsythe test). For 1 cm axon density data, when the Brown-Forsythe test failed, the Welch's test was run, which showed no significance. Cohen's effect size was calculated to be $d = 1.41$ for 1 cm TENG Health; $d = 1.95$ for axon density; $d = 0.43$ for fascicle diameter; $d = 1.64$ for TENG health; $d = 0.80$ for axon density; and $d = 1.49$ for fascicle diameter.

Chronic morphometry. Axial sections taken distal to the repair zone were labeled for the axonal marker neurofilament and myelin marker myelin basic protein (MBP), as described above, to count myelinated axons. The number of axons, axon diameter, and g-ratio of axons—indicative of extent of axon myelination—in each fascicle of each nerve was counted using Fiji. All images for quantification were acquired by setting initial acquisition settings to show maximum morphological clarity, and acquisition as well as analysis settings were kept consistent across images for quantification. In brief, the g-ratio was calculated by measuring the ratio of the inner diameter (unmyelinated axon) to outer diameter (myelinated axon); see Katiyar *et al.*³⁸ for details. The effect of TENG type on morphological regenerative outcomes (host axon count, diameter, and myelination) was assessed. All chronic morphometry data passed the Brown-Forsythe test showing equal variances and significance was tested using one-way ANOVA tests. Cohen's effect size was calculated to be $d = 2.26$ for host axon count; $d = 0.17$ for average axon diameter; and $d = 1.06$ for G-Ratio.

Statistical analyses. For all quantitative measures, the group mean, standard deviation, and standard error of the mean were calculated for each group. When significant differences were detected between groups using one-way ANOVA tests, Tukey's *post hoc* comparisons test was performed. For all statistical tests, $p < 0.05$ was required for significance. Statistical testing was performed using GraphPad Prism version 8.0.2 (GraphPad Software, La Jolla, CA).

Results

Absence of Gal in nerves of GalSafe pigs

SCNT and gene editing techniques were used to disrupt one allele of the $\alpha 1,3$ -galactosyltransferase ($\alpha 1,3$ GT) gene, which is known to synthesize Gal epitopes.³⁰ Bacterial toxins were then used to target cells containing the second allele.²¹ A male and female heterozygous knockout pig were bred to produce embryos containing WT, SKO, and DKO pigs.²¹ Phenotyping was done after embryo collection to determine whether an individual embryo was WT, SKO, or DKO. Before breeding GalSafe pigs, the knockdown of Gal in adult pigs was confirmed. Positive expression of Gal was observed through the presence of lectin staining (brown) in adult WT pig nerves, whereas the absence of lectin staining, and therefore Gal expression, was observed in genetically engineered adult DKO GalSafe pigs (Fig. 2). This verified that Gal knockdown extended to peripheral nerves, thereby confirming that neurons isolated from GalSafe pigs would provide a Gal-negative starting biomass for TENG fabrication.

Culture and characterization of GalSafe neurons

GalSafe sensory DRG, dissociated motor neurons, and aggregated motor neurons were cultured out to 14 days. Cell health was monitored over the 14 DIV, with axon outgrowth indicative of cell health. Robust axon outgrowth was observed over time in all cultures, but was greatest in sensory DRG and aggregated motor neurons (Fig. 3A, C). In DRG cultures, axon length appeared to increase significantly by 5 DIV ($****p < 0.0001$; Fig. 3C) and remained unchanged out to 14 DIV. This does not implicitly mean that axons did not grow after 5 DIV, it is mostly due to restrictions in plating area and the field of view during imaging. In addition, as

expected, axon outgrowth in motor neurons was greater when they were aggregated, with motor neuron aggregates exhibiting significantly increased axon length compared to time-matched dissociated motor neurons at 8 and 15 DIV ($##p < 0.01$, $###p < 0.001$; Fig. 3C). Immunolabeling for neuronal markers confirmed neuronal phenotype through positive labeling for the axonal marker, β -tubulin III (green) in all cell types and positive expression for the motor neuron marker ChAT (red) in motor neuron cultures, and showed the minimal presence of contaminating glial cells (GFAP, red) in DRG (Fig. 3B, D).

Axonal stretch growth from GalSafe neurons

Axons of sensory DRG and motor neuron aggregates were successfully stretch-grown to produce pure sensory as well as mixed motor-sensory axon tracts spanning 1 cm. Following 1 cm stretch growth, GalSafe neurons produced robust, continuous, healthy axon tracts, with axon density (WT: 92.06 ± 1.954 axons; SKO: 81.61 ± 9.3 axons; DKO: 57.39 ± 17.75 axons), fascicle diameter (WT: $7.157 \pm 0.6584 \mu\text{m}$; SKO: $6.183 \pm 1.417 \mu\text{m}$; DKO: $6.328 \pm 0.9361 \mu\text{m}$), and health (TENG health score for WT: 4.750 ± 0.1443 ; SKO: 4.125 ± 0.2394 ; DKO: 3.875 ± 0.375) statistically equivalent to WT (i.e., non-GalSafe) neurons, regardless of phenotype—SKO or DKO GalSafe (Fig. 4). Determination of axon health was done on a semiquantitative scale, ranging from 1 (unhealthy) to 5 (very healthy), and took into account continuity of axons, density of axons, as well as proteinaceous build-up along axon tracts that may indicate early degeneration. Since no differences between cell phenotypes was observed, future assessment of axon tracts at longer lengths combined SKO and DKO data as simply GalSafe.

Following 1 cm stretch growth, we found that GalSafe axons were also able to withstand stretch growth of up to 5 cm, producing healthy, aligned axon tracts. Vigorous axon fasciculation, or bundling, was evident in 3 cm and 5 cm long axon tracts (Fig. 5A–F). In addition, positive β -tubulin III labeling confirmed no noticeable change in neuronal phenotype as a result of longer stretch growth paradigms and was clearly indicative of continuous axons spanning 3 cm (Fig. 5G), with axon density (1 cm: $69.5\% \pm 10.3\%$; 3 cm:

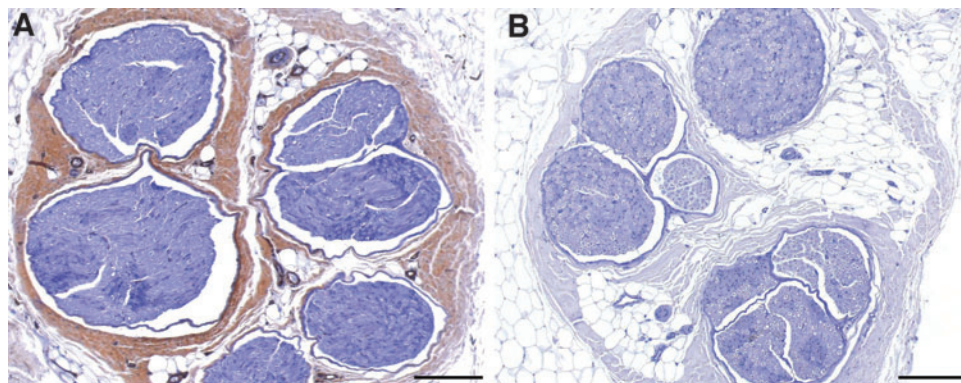


FIG. 2. GalSafe nerve is Gal null. Immunohistochemical staining with GS-Ib₄ isolectin (Lectin) of nerve tissue from (A) WT (nonengineered) and (B) GalSafe pig. Lectin (brown stain) is well established to have a high affinity to bind to gal epitopes. (A) Nonengineered nerve shows gal is present and highly concentrated in the neurolemma. (B) Lectin staining was not present in the GalSafe nerve, indicating absence of gal. Scale: 200 μm . WT, wild type. Color images are available online.

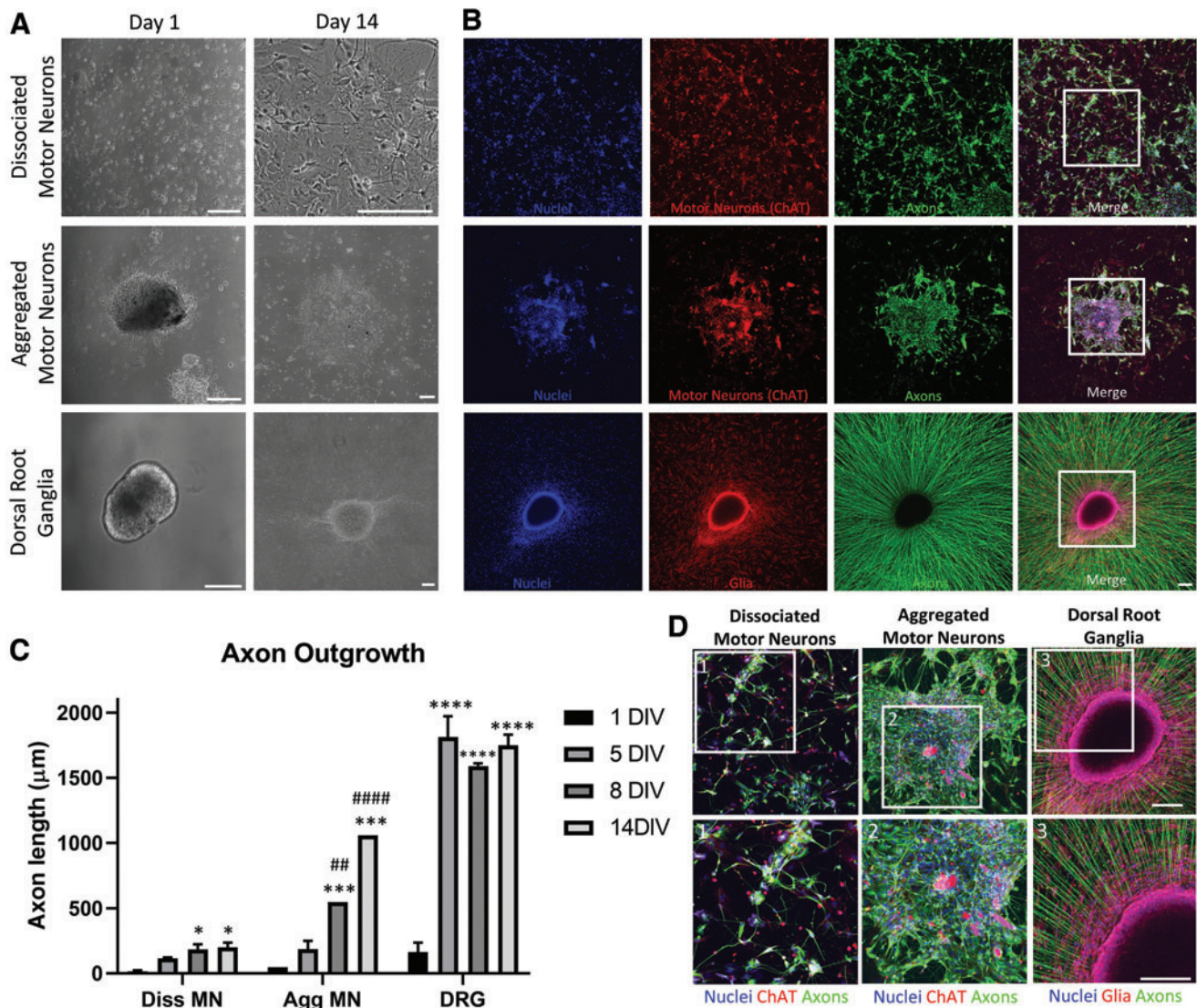


FIG. 3. Characterization of GalSafe neurons. **(A)** Phase contrast images showing GalSafe dissociated motor neurons, aggregated motor, and sensory DRG at 1 and 14 DIV. Importantly, robust axon outgrowth is observed by 14 DIV in all cell types. **(B)** Immunolabeling of GalSafe neurons at 9 DIV confirms neuronal phenotype, as indicated by positive β -tubulin III expression (*green*), motor neuron phenotype for the corresponding dissociated and forced aggregated motor neuron cultures (ChAT, *red*), as well as contaminating glia in DRG cultures (GFAP, *red*). **(C)** Increased axon outgrowth was observed over time with statistically significant axon outgrowth seen in dissociated motor neurons and DRG compared to 1 DIV ($*p < 0.05$, $***p < 0.001$, $****p < 0.0001$). In addition, increased axon outgrowth at 8 and 14 DIV in aggregated motor neurons compared to dissociated motor neurons was observed ($##p < 0.01$, $####p < 0.0001$). Error bars represent SEM. **(D)** Higher magnification confocal reconstructions of dissociated motor neurons, aggregated motor neurons, and DRG from **(A)**, with **(1–3)** showing further zoom-ins of selected regions for clarity. Scale: 250 μ m. ChAT, choline acetyl transferase; DIV, days *in vitro*; GFAP, glial fibrillary acidic protein. Color images are available online.

67.4% \pm 4.4%; 5 cm: 49.6% \pm 8.1%) and health score remaining statistically equivalent with increased length of axons (Fig. 5H–K). An increase in the number of larger fascicles was observed with increasing axon tract length (Fig. 5M–O). Importantly, the novel GalSafe TENGs exhibited statistically equivalent TENG health compared to WT TENGs (Fig. 5L). These results confirm that clinical-grade GalSafe neurons are able to withstand our stretch growth paradigm to produce ultralong axon tracts spanning 5 cm in a relatively short time (23 days), with longer lengths possible.

Transplantation of GalSafe TENGs into a rodent model of PNI

Following successful stretch growth of GalSafe axons, the axon tracts were encapsulated in an ECM for stabilization and protection, transferred into a NGT (Fig. 1D) and transplanted into a 1.0cm sciatic nerve lesion in an athymic rat. Both sensory-only as well as mixed-motor sensory TENGs were transplanted *in vivo*. At the acute time point of 2 weeks posttransplantation, survival of the xenogeneic porcine GalSafe TENG neurons was observed regardless of neuronal

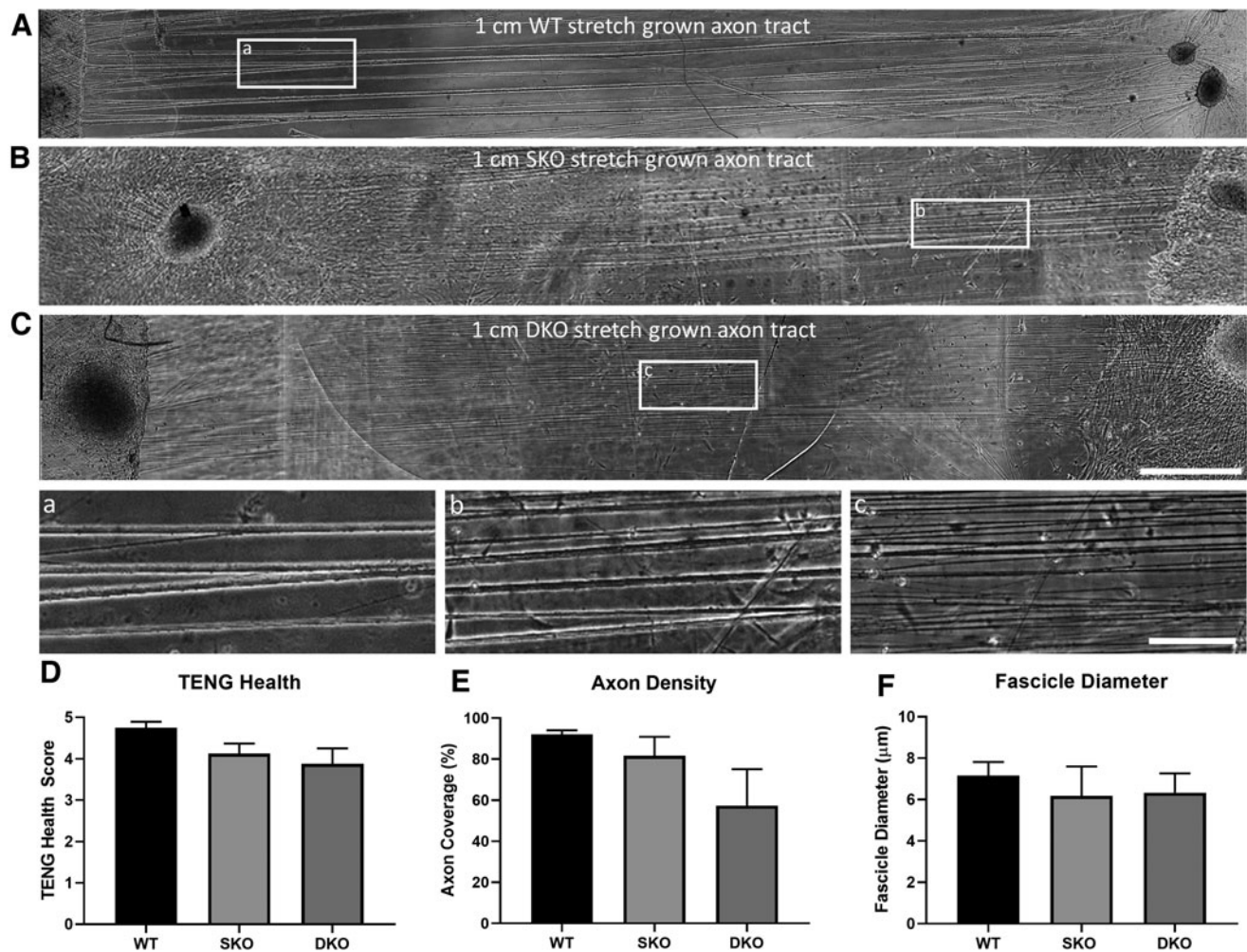


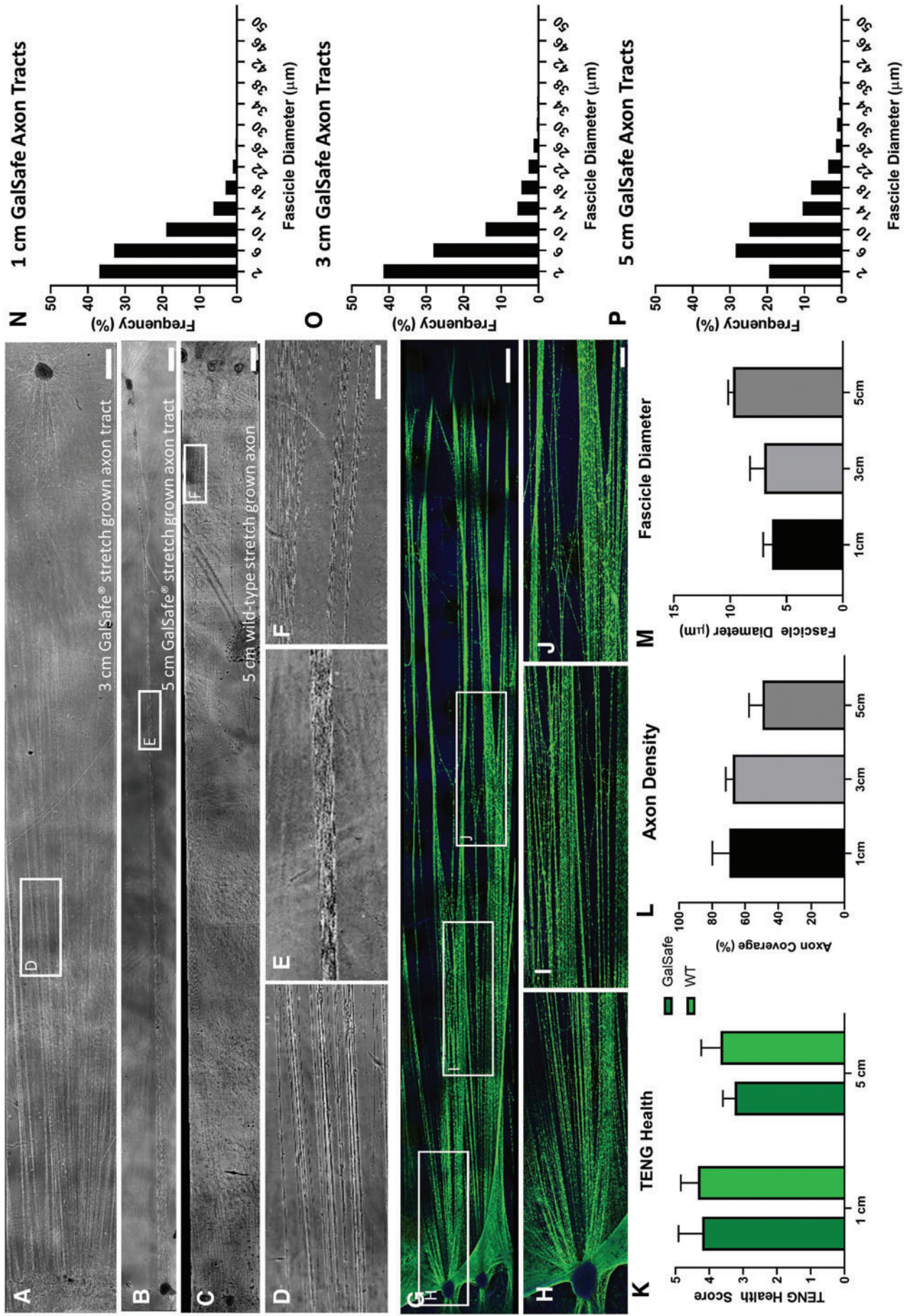
FIG. 4. Successful stretch growth of GalSafe neurons to 1 cm. Stretch growth of (A) WT, (B) SKO, and (C) DKO DRG to 1 cm exhibits healthy axons tracts (a–c) zoom-in regions of axons, with similar (D) TENG health, based on a semiquantitative score that takes into account axon density and individual axon/fascicle health scored on a scale of 1 (worst) to 5 (best) (see Table 1 for description of scoring scale; WT vs. SKO, $p=0.2804$; WT vs. DKO, $p=0.1085$; SKO vs. DKO, $p=0.7945$), (E) axon density of stretch-grown axons over a 1 cm area (WT vs. SKO, $p=0.8046$; WT vs. DKO, $p=0.1429$; SKO vs. DKO, $p=0.3477$), and (F) stretch-grown fascicle diameter ($p>0.82$) ($n=4$ each). Scale: (A–C) 1000 μm ; (a–c) 250 μm . DKO, double-knockout; SKO, single-knockout.

phenotype (SKO or DKO) and TENG modality (sensory or mixed motor sensory) (Fig. 6A, B). Furthermore, host axons (red) were seen to grow directly along transplanted GalSafe axons, indicating that the mechanism of AFAR that was observed in earlier studies upon allogeneic transplantation of WT TENGs (i.e., rat TENGs into rat and pig TENGs into pig) was maintained here with xenogeneic transplantation of por-

phine GalSafe TENGs into athymic rats (Fig. 6). In addition, robust Schwann cell (far red) infiltration into the graft zone was also seen in all TENG types (Fig. 6). The survival of xenogeneic GalSafe TENGs and maintenance of AFAR is an important first step in the validation of GalSafe TENGs.

At the chronic time point of 8 weeks, regenerated axons were found in the nerve segment 5 mm distal to the injury

FIG. 5. GalSafe axons stretch-grown to 5 cm. GalSafe DRG axons were successfully stretch-grown to (A) 3 cm and (B) 5 cm, exhibiting robust axon elongation similar to (C) WT axon tracts spanning 5 cm. Zoom in regions from (A–C) show intact, healthy axons from (D) 3 cm, and (E) 5 cm GalSafe stretch-grown constructs compared to (F) 5 cm WT stretch-grown constructs. (G) Ultra-long GalSafe stretch-grown constructs positively labeled for the neuronal marker β -tubulin III. (H–J) Zoom-in regions showing axon structure. (K) No significant adverse effects were seen on TENG health up to 5 cm. No significant differences were found in (L) axon density over the culture area ($p>0.6155$ between groups) or (M) fascicle diameter due to axon length (1 cm vs. 3 cm, $p=0.9076$; 1 cm vs. 5 cm, $p=0.1479$; 3 cm vs. 5 cm, $p=0.4222$; $n=8$ for 1 cm GalSafe; $n=6$ for 1 cm WT; $n=3$ for 3 cm GalSafe; $n=2$ for 5 cm GalSafe; and $n=3$ for 5 cm WT). Histograms showing axon diameter frequency for (N) 1 cm, (O) 3 cm, and (P) 5 cm axon tracts show an increase in the proportion of larger fascicles with increased axon length. (A–C) Scale 1000 μm ; (D–F) 500 μm ; (G) 1000 μm ; (H–J) 500 μm . Color images are available online.



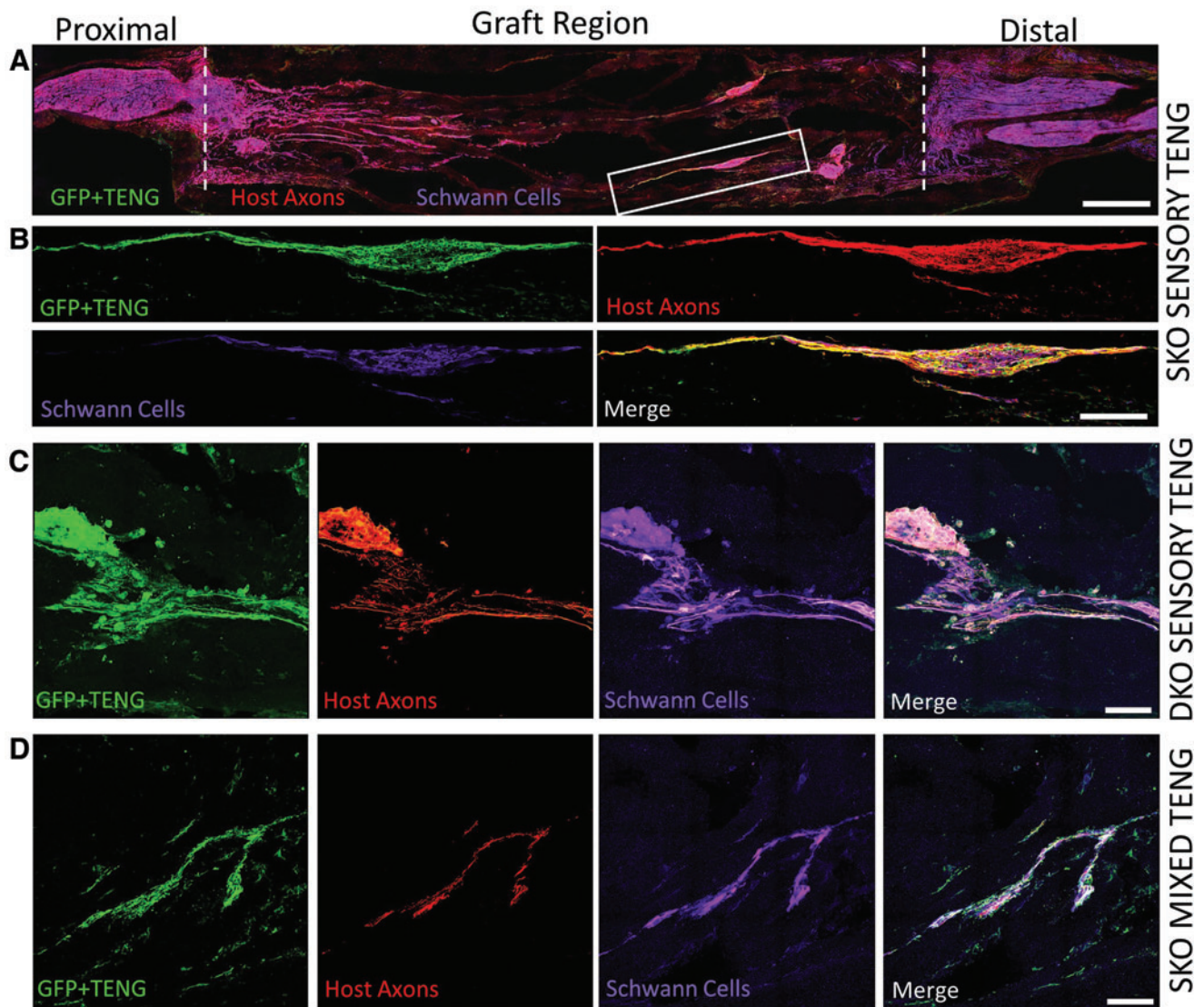


FIG. 6. GalSafe TENGs survive *in vivo* following bridging of segmental nerve defects in athymic rats. TENG survival and evidence of AFAR was seen 2 weeks following transplantation of GalSafe TENGs to repair a 1.0 cm lesion in the sciatic nerve of athymic rats. (A) Example of a longitudinal nerve section following transplantation of a SKO sensory TENG. Dashed lines indicate proximal nerve stump, graft region, and distal nerve stump. Zoom in confocal reconstructions of nerve lesions clearly show evidence of AFAR following repair with (B) SKO sensory TENG, (C) DKO sensory TENG, and (D) SKO mixed motor-sensory TENG. In all groups, axons (neurofilament; red) were found growing along transplanted TENG neurons/axons (GFP+) as well as directed Schwann cell (S100; far red) infiltration into the graft zone, confirming that the mechanism of AFAR was maintained via GalSafe TENGs. Scale: (A) 1000 μm ; (B) 250 μm , (C, D) 100 μm . AFAR, axon-facilitated axon regeneration. Color images are available online.

in all repair groups, with the appearance of more mature, myelinated axons following TENG (regardless of phenotype, e.g., mixed or sensory TENGs and/or SKO or DKO neurons) and autograft repair (Fig. 7A–D). Furthermore, repair with TENGs (mean: 5401 ± 2116 host axons) and autografts (mean: 9002 ± 841 host axons) appeared to result in greater axon counts in the distal stump as well as larger axons and more optimal g-ratios (a measure of myelination), compared to repair with NGTs (mean: 2687 ± 466 host axons) (Fig. 7E–G). Notably, the g-ratio for the NGT repair group had the greatest deviation from the reportedly optimal value of 0.6 (mean NGT g-ratio: 0.7). Importantly, these

results confirm that GalSafe TENGs survive *in vivo* at chronic time points and promote regeneration similarly to previously studied WT TENGs.

Discussion

PNI remains a major medical concern, with over 550,000 corrective surgical procedures every year in the United States alone, often resulting in unsatisfactory functional outcomes even with current gold standard treatment.^{31,47–49} Notably, functional recovery is considered “successful” if the patient regains the ability to move the limb against

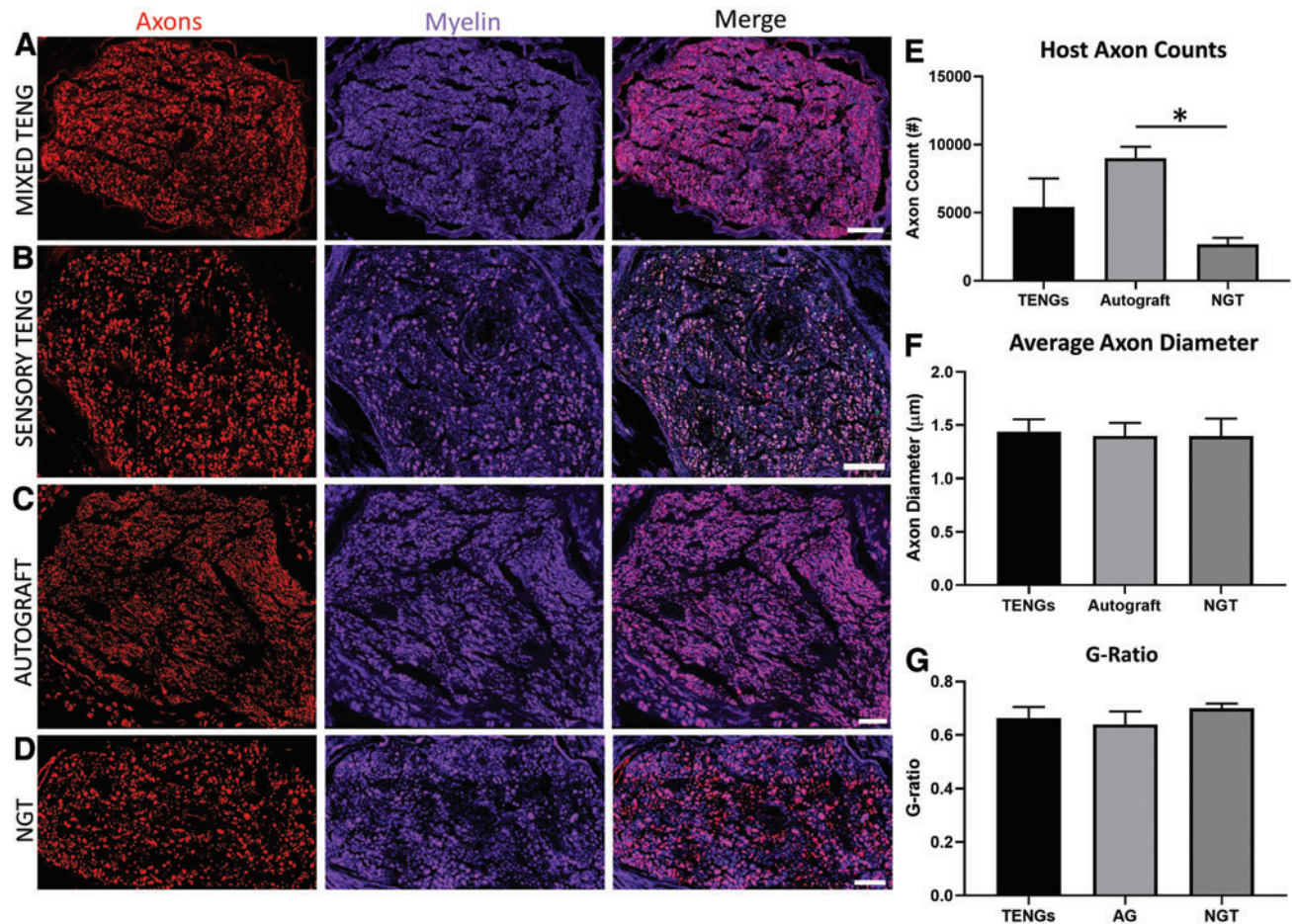


FIG. 7. GalSafe TENGs promote host axon regeneration. At 8 weeks posttransplantation, the distal nerve segment was assessed for evidence of host axon regeneration. Axial sections of the distal nerve exhibited high numbers of myelinated host axons following (A) mixed GalSafe TENG, (B) sensory GalSafe TENG, (C) autograft, and (D) NGT repair. (E) Quantification of number of axons 5 mm distal to the injury site revealed increased axon counts in TENG and autograft repair groups, with significantly increased axon counts in the autograft repair group compared to NGT repair ($*p < 0.05$). However, no significant effect on (F) host axon diameter or (G) g-ratio was seen regardless of repair strategy. Scale: 50 μm . Color images are available online.

gravity. However, this metric still leaves debilitated patients dependent on caretakers, thus generally resulting in decreased quality of life. Current treatment for segmental PNI relies on one of two general strategies (1) grafting of non-living material (i.e., ANAs or biomaterial-based NGTs) or (2) autografts, which are natural living scaffolds, since they contain numerous host Schwann cells and other proregenerative features, such as the formation of proregenerative bands of Bungner. While the living autograft is markedly superior to nonliving/acellular options, the act of harvesting an autograft deliberately causes a deficit in the patient, results in undesirable scarring, may lead to the formation of a painful neuroma, and may not provide enough material for long-gap or polytrauma scenarios. Therefore, the field is in desperate need for a bioengineered TEMP that meets—but ideally exceeds—the regenerative performance of the so-called “gold standard” autograft. Here, a cell-based and/or tissue-engineering approach to nerve repair that is able to actively direct axon regeneration instead of serving as a passive substrate holds the potential to transform nerve repair procedures and recovery. To this end, we have de-

veloped TENGs that are comprised of living, three-dimensional axon tracts that are able to actively drive and sustain host regeneration. TENGs, by way of their axon tracts, are able to respond to the host environment and present the necessary cues to directly guide regenerating axons and host Schwann cells to achieve increased levels of functional recovery.³⁵

While tissue-engineered therapeutics may prove transformational in treating many types of disorders and deficits, several key considerations must be taken into account for biomanufacturing of this class of therapeutics. First and foremost, is choosing the starting biomass, which must prove suitable in serving as a building block for the desired TEMP and must be safe, readily available, and cost effective. In this study, we have achieved an important step toward clinical-grade biomanufacturing of TENGs by recapitulating axon stretch growth up to 5 cm using a clinically viable starting biomass procured from genetically engineered pigs. We have shown that GalSafe DRG can be harvested and cultured, yielding viable neurons with extensive neurite outgrowth. Similarly, GalSafe motor neurons were

acquired and dissociated from the spinal cord, and then force aggregated to form an engineered “ganglia” that mimicked the general structure of DRG. This aggregation resulted in more robust axon outgrowth that was greater than that seen in dissociated motor neuron cultures and was similar to DRG neurite outgrowth. GalSafe axons, regardless of phenotype (i.e., SKO vs. DKO), were then successfully stretch-grown, producing healthy TENGs with axon tracts spanning up to 5 cm following the stretch growth paradigm used previously for WT porcine neurons (as well as from numerous other neuronal sources). The process of axon stretch growth has been seen to increase fasciculation, or bundling, of axons to form thick axon fascicles.^{38,39} This increase in fasciculation, as seen by a shift to the right (i.e., larger diameter axons/fascicles) (Fig. 5N–P), is directly related to the increasing average axon diameter as axon tract length increases over time (Fig. 5M). Importantly, the decrease in axon density as axon tract length increases from 1 to 5 cm, is not indicative of a decrease in axon number, but is due to increased axon fasciculation.

After successfully stretch-growing axons, TENGs were transplanted into a PNI model in athymic rats. Upon transplantation of mixed motor-sensory and sensory-only GalSafe TENGs into athymic rats, TENG survival and host axon regeneration was confirmed at the acute time point of 2 weeks as well as chronic time point of 8 weeks. Host axon regeneration was measured by quantifying the number, diameter, and g-ratio of regenerated host axons in the distal nerve stump (Fig. 7E–G). The g-ratio measures myelination of axons and is a ratio of axon diameter to myelinated axon diameter. The optimal g-ratio value for myelination of a healthy axon is ~0.6, however, the g-ratio is generally observed to be slightly higher in the peripheral nervous system (PNS).⁵⁰ While g-ratios for all groups were slightly >0.6, the mean g-ratio for the NGT repair group exhibited a larger increase from the optimal g-ratio value than TENG or autograft repair, suggesting suboptimal and/or delayed regeneration in the NGT group. In addition, it is possible that at this time point of 8 weeks, the regenerative process was still early and the axons were temporarily over-myelinated.⁵⁰ Overall, this study confirms that the TENG Mechanism of Action (MoA) and functionality were maintained when GalSafe neurons were used for TENG biofabrication.

Revivicor, Inc., has utilized SCNT and gene targeting techniques to establish GalSafe pigs as a genetically engineered pig line that has no detectable Gal present.²⁸ Revivicor accomplished this via disruption of the pig GGTA1 locus, which was verified to result in homozygous inactivation of both alleles of GGTA1 and lack of Gal expression/presence in these pigs (Fig. 2). These pigs are intended to provide a source of raw materials for fabrication and distribution of implantable medical products for human use. Studies have demonstrated that tissue harvested from GalSafe animals did not express detectable levels of Gal, whereas Gal was easily detected in comparable non-engineered pig tissue,⁵¹ and that the Gal expression levels in GalSafe animals was comparable to that of catarrhines.⁵² Interestingly, GalSafe pigs also provide a source of meat for human consumption for those affected by meat allergies driven by the presence of Gal on nonengineered pig tissue. Along with IgG and IgM antibodies, allergists have described large populations with high titers of anti-Gal IgE

that appear to be initiated by arachnid bites.^{53–55} IgE antibodies have specificity to a unique antigen and are responsible for allergic responses that include anaphylactic shock. Exposure to α -Gal via inhalation, dermal contact, consumption, injection, or implantation of mammalian-derived products has been well documented to result in adverse events, including anaphylactic shock to α -Gal sensitized populations.^{54,56–61} Anaphylaxis triggered by exposure to α -Gal was reported to be more prevalent than all other food allergens combined.⁶² Most relevant to the current work, tissue derived from GalSafe pigs may primarily act as a temporary scaffold that retains many endogenous factors to promote healing and/or recellularization with host cells; indeed, most grafts have been found to remodel between 1 and 3 months (depending on graft size/length). GalSafe tissue grafts are commonly regarded as immunogenically quiescent and therefore type-matching or the use of immunosuppressive drugs is not required.

Through the strides made by Revivicor, Inc., in producing GalSafe pigs, our team has taken advantage of utilizing a safe xenogeneic cell source for eventual clinical-grade manufacturing of TENGs. GalSafe neurons pose many advantages over the use of other commonly used cell types for starting biomass (i.e., human stem cells). These include a large supply of terminally differentiated neurons that do not require weeks to months of differentiation and addition of costly growth factors. Xenogeneic primary cell sources are also more homogenous populations of cells than stem cells, as batch-to-batch variability due to differentiation is eliminated. Dependent on the exact tissue of isolation, in the case of acquiring terminally differentiated cells (as opposed to acquiring immature stem cells, or de-differentiating to induce stem cell behavior), the potential for tumorigenesis following transplantation is effectively nil. Finally, stem cell-differentiated neurons appear unable to tolerate equivalent strain rates as embryonic primary neurons, leading to less robust stretch growth and lower quality TENGs when fabricated from stem cell-derived neurons.⁴¹ While xenogeneic cells may present risks associated with a human immune response, GalSafe tissue has proven to be safe and substantially equivalent to nonengineered pig tissue except for the intended design (absence of Gal) in various *in vivo* studies, with no morbidity or mortality attributed to implants derived from α -Gal knockout pigs.^{63–65} Previous analysis of hematology and serum chemistry of genetically engineered pigs, including GalSafe pigs, concluded that genetic modification of the pig does not result in hematologic or biochemical parameters that are considered harmful to the animal.⁶ In addition, no differences in tissue matrices and structural integrity and function of the ECM has been observed.^{51,66,67} Fortunately, TENGs are intended to act as a temporary scaffold to drive host nerve regeneration and potentially prolong the regenerative distal nerve environment.^{37,68} While GalSafe cells are not expected to elicit an immune response, and the presence of T cells should not directly affect the integration, functionality, or MoA of TENGs, mild immunosuppression may be administered as a precaution so that T cells do not affect TENG health and survival as this may affect integration, functionality, and MoA of the TENGs. Once the nerve has sufficiently regenerated, any mild immunosuppression that may have been administered can be gradually terminated resulting in degradation or resorption of the TENG material.

Importantly, there are considerations with our *in vivo* model that limit the relevance of our findings. Notably,

transplantation of tissue engineered products into athymic rats is a routine first step in testing the TEMP before advancing to larger animal models. These rats lack functionally mature T cells, which healthy humans possess. However, as noted above, the presence of T cells should not directly affect TENG efficacy. The results of our experiments show that GalSafe neurons provide suitable starting biomass for TENGs and that GalSafe TENGs survive and support axonal regeneration when transplanted into an athymic rat model of PNI. The clinical product will likely be DKO mixed motor-sensory TENGs, as the presence of motor neurons is believed to result in increased motor axon growth both in development and post-injury.^{38,69,70} We included SKO cells in our transplant studies to determine whether there was an effect of single or double allele knockdown (i.e., SKO or DKO, respectively). Of note, our goal for *in vivo* testing was not to perform a full efficacy study, rather our goals were (1) to ensure that GalSafe TENGs survived post-implant, (2) that the MoA observed with WT TENGs was conserved in Gal-Safe TENGs, and (3) that GalSafe TENGs supported axon regeneration across the graft zone. Having successfully demonstrated these points for TENGs, future work will determine the efficacy of GalSafe TENGs in an immunocompetent large animal model that more closely resembles the human PNS to determine long-term safety and efficacy, as well as the cell fate of GalSafe TENGs. Our biomanufacturing efforts will focus on biopreservation, QA, and quality control attributes, as well as release criteria for TENGs based on nondestructive testing outcomes. In addition, the use of GalSafe cells will allow a more streamlined path to achieving full cGMP production of TENGs, as Revivicor has advanced the regulatory approval of the GalSafe pig for human use through the U.S. FDA to complement Axonova's efforts to gain regulatory approval for TENGs. These steps will streamline the path toward achieving full cGMP production of GalSafe TENGs, clearing the way for pivotal safety and efficacy testing of GalSafe TENGs as an off-the-shelf alternative to autografts.

Disclosure Statement

D.K.C., D.H.S., and H.C.L. are cofounders and K.S.K. is currently an employee of Axonova Medical, LLC, which is a University of Pennsylvania spin-out company focused on translation of advanced regenerative therapies to treat nervous system disorders. Multiple patents relate to the composition, methods, and use of TENGs, including U.S. Patent 6,264,944 (D.H.S.), U.S. Patent 6,365,153 (D.H.S.), U.S. Patent 9,895,399 (D.H.S. and D.K.C.), U.S. Patent 10,525,085 (D.H.S. and D.K.C.), U.S. Provisional Patent 62/569,255 (D.K.C.), U.S. Provisional Patent 62/936,983 (D.K.C. and J.C.B.), and U.S. Provisional Patent 62/937,489 (D.K.C. and J.C.B.). J.R.B., A.W., and D.L.A. are employees of Revivicor, Inc., a wholly owned subsidiary of United Therapeutics, Inc. No other author has declared a potential conflict of interest.

Funding Information

Financial support provided by the National Institutes of Health (SBIR R43 No. NS108869 [H.C.L. and D.K.C.]) and the Department of Defense (CDMRP/JPC8-CRMRP No. W81XWH-16-1-0796 [D.K.C.]).

References

- Cozzi, E., and White, D.J. The generation of transgenic pigs as potential organ donors for humans. *Nat Med* **1**, 964, 1995.
- Godehardt, A.W., and Tönjes, R.R. Xenotransplantation of decellularized pig heart valves—regulatory aspects in Europe. *Xenotransplantation* **27**, e12609, 2020.
- Onions, D., Cooper, D.K., Alexander, T.J., *et al.* An approach to the control of disease transmission in pig-to-human xenotransplantation. *Xenotransplantation* **7**, 143, 2000.
- Sykes, M., and Sachs, D.H. Transplanting organs from pigs to humans. *Sci Immunol* **4**, 1, 2019.
- Cooper, D.K., Gollackner, B., and Sachs, D.H. Will the pig solve the transplantation backlog?. *Annu Rev Med* **53**, 133, 2002.
- Ekser, B., Ezzelarab, M., Hara, H., *et al.* Clinical xenotransplantation: the next medical revolution?. *Lancet* **379**, 672, 2012.
- Graham, M.L., Bellin, M.D., Papas, K.K., Hering, B.J., and Schuurman, H.J. Species incompatibilities in the pig-to-macaque islet xenotransplant model affect transplant outcome: a comparison with allotransplantation. *Xenotransplantation* **18**, 328, 2011.
- Ekser, B., Rigotti, P., Gridelli, B., and Cooper, D.K. Xenotransplantation of solid organs in the pig-to-primate model. *Transpl Immunol* **21**, 87, 2009.
- Source Animal, Preclinical, and Clinical Issues Concerning the Use of Xenotransplantation Products in Humans—Guidance for Industry, U.S. Department of Health and Human Services, Food and Drug Administration. Center for Biologics Evaluation and Research, 2016.
- Elliott, R., Escobar, L., Tan, P., *et al.* Intraperitoneal alginate-encapsulated neonatal porcine islets in a placebo-controlled study with 16 diabetic cynomolgus primates. *Transplant Proc* **37**, 3505, 2005.
- Garkavenko, O., Croxson, M., Irgang, M., Karlas, A., Denner, J., and Elliott, R. Monitoring for presence of potentially xenotic viruses in recipients of pig islet xenotransplantation. *J Clin Microbiol* **42**, 5353, 2004.
- Garkavenko, O., Wynyard, S., Nathu, D., *et al.* Porcine endogenous retrovirus (PERV) and its transmission characteristics: a study of the New Zealand designated pathogen-free herd. *Cell Transplant* **17**, 1381, 2008.
- Schuurman, H.-J. Regulatory aspects of clinical xenotransplantation. *Int J Surg* **23**, 312, 2015.
- V. Corporation, BLA Clinical Review Memorandum—MACI, 2016.
- O. Inc., Summary of Safety and Effectiveness Data, FDA, 1998.
- Galili, U. The α -gal epitope and the anti-Gal antibody in xenotransplantation and in cancer immunotherapy. *Immunol Cell Biol* **83**, 674, 2005.
- Galili, U. Anti-Gal: an abundant human natural antibody of multiple pathogeneses and clinical benefits. *Immunology* **140**, 1, 2013.
- Joziasse, D.H., Shaper, J. Van den Eijnden, D. Van Tunen, A., and Shaper, N. Bovine alpha 1—3-galactosyltransferase: isolation and characterization of a cDNA clone. Identification of homologous sequences in human genomic DNA. *J Biol Chem* **264**, 14290, 1989.
- Kobayashi, T., and Cooper, D.K. Anti-Gal, α -Gal epitopes, and xenotransplantation, α -Gal and anti-Gal. *Subcell Biochem* **32**, 229, 1999.
- Macher, B.A., and Galili, U. The Gal α 1, 3Gal β 1, 4GlcNAc-R (α -Gal) epitope: a carbohydrate of unique

- evolution and clinical relevance. *Biochim Biophys Acta* **1780**, 75, 2008.
21. Phelps, C.J., Koike, C., Vaught, T.D., *et al.* Production of $\alpha 1$, 3-galactosyltransferase-deficient pigs. *Science* **299**, 411, 2003.
 22. Galili, U., and Swanson, K. Gene sequences suggest inactivation of alpha-1, 3-galactosyltransferase in catarrhines after the divergence of apes from monkeys. *Proc Natl Acad Sci U S A* **88**, 7401, 1991.
 23. Sandrin, M.S., and McKenzie, I. Gal alpha (1, 3) Gal, the major xenoantigen(s) recognised in pigs by human natural antibodies. *Immunol Rev* **141**, 169, 1994.
 24. Galili, U., Shohet, S.B., Kobrin, E., Stults, C.L., and Macher, B.A. Man, apes, and Old World monkeys differ from other mammals in the expression of alpha-galactosyl epitopes on nucleated cells. *J Biol Chem* **263**, 17755, 1988.
 25. Oriol, R., Candelier, J.J., Taniguchi, S., *et al.* Major carbohydrate epitopes in tissues of domestic and African wild animals of potential interest for xenotransplantation research. *Xenotransplantation* **6**, 79, 1999.
 26. Joziase, D.H., and Oriol, R. Xenotransplantation: the importance of the Galalpha1,3Gal epitope in hyperacute vascular rejection. *Biochim Biophys Acta* **1455**, 403, 1999.
 27. Ezzelarab, M., Garcia, B., Azimzadeh, A., *et al.* The innate immune response and activation of coagulation in alpha1,3-galactosyltransferase gene-knockout xenograft recipients. *Transplantation* **87**, 805, 2009.
 28. Ekser, B., Bianchi, J., Ball, S., *et al.* Comparison of hematologic, biochemical, and coagulation parameters in alpha1,3-galactosyltransferase gene-knockout pigs, wild-type pigs, and four primate species. *Xenotransplantation* **19**, 342, 2012.
 29. Bianchi, J., Walters, A., Fitch, Z.W., and Turek, J.W. Alpha-gal syndrome: implications for cardiovascular disease. *Glob Cardiol Sci Pract* **2019**, 1, 2019.
 30. Dai, Y., Vaught, T.D., Boone, J., *et al.* Targeted disruption of the alpha1,3-galactosyltransferase gene in cloned pigs. *Nat Biotechnol* **20**, 251, 2002.
 31. Robinson, L.R. Traumatic injury to peripheral nerves. *Muscle Nerve* **23**, 863, 2000.
 32. Grinsell, D., and Keating, C. Peripheral nerve reconstruction after injury: a review of clinical and experimental therapies. *Biomed Res Int* **2014**, 698256, 2014.
 33. Lee, S.K., and Wolfe, S.W. Peripheral nerve injury and repair. *J Am Acad Orthop Surg* **8**, 243, 2000.
 34. Tubbs, R.S., Rizk, E., Shoja, M.M., Loukas, M., Barbaro, N., and Spinner, R.J. *Nerves and Nerve Injuries: Vol 2: Pain, Treatment, Injury, Disease and Future Directions*. Academic Press, 2015.
 35. Maggiore, J.C., Burrell, J.C., Browne, K.D., *et al.* Tissue engineered axon-based "living scaffolds" promote survival of spinal cord motor neurons following peripheral nerve repair. *JTERM* **14**, 1892, 2020.
 36. Pfister, B.J., Iwata, A., Taylor, A.G., Wolf, J.A., Meaney, D.F., and Smith, D.H. Development of transplantable nervous tissue constructs comprised of stretch-grown axons. *J Neurosci Methods* **153**, 95, 2006.
 37. Katiyar, K.S., Struzyna, L.A., Morand, J.P., *et al.* Tissue engineered axon tracts serve as living scaffolds to accelerate axonal regeneration and functional recovery following peripheral nerve injury in rats. *Front Bioeng Biotechnol* **8**, 492, 2020.
 38. Katiyar, K.S., Struzyna, L.A., Das, S., and Cullen, D.K. Stretch growth of motor axons in custom mechanobioreactors to generate long-projecting axonal constructs. *J Tissue Eng Regen Med* **13**, 2040, 2019.
 39. Pfister, B.J., Iwata, A., Meaney, D.F., and Smith, D.H. Extreme stretch growth of integrated axons. *J Neurosci* **24**, 7978, 2004.
 40. Smith, D.H., Wolf, J.A., and Meaney, D.F. A new strategy to produce sustained growth of central nervous system axons: continuous mechanical tension. *Tissue Eng* **7**, 131, 2001.
 41. Chen, H.I., Jgamadze, D., Lim, J., *et al.* Functional cortical axon tracts generated from human stem cell-derived neurons. *Tissue Eng Part A* **25**, 736, 2019.
 42. Huang, J.H., Zager, E.L., Zhang, J., *et al.* Harvested human neurons engineered as live nervous tissue constructs: implications for transplantation. *J Neurosurg* **108**, 343, 2008.
 43. Graber, D.J., and Harris, B.T. Purification and culture of spinal motor neurons from rat embryos. *Cold Spring Harb Protoc* **2013**, 319, 2013.
 44. Ungrin, M.D., Joshi, C., Nica, A., Bauwens, C., and Zandstra, P.W. Reproducible, ultra high-throughput formation of multicellular organization from single cell suspension-derived human embryonic stem cell aggregates. *PLoS One* **3**, e1565, 2008.
 45. Zimmermann, J.A., and McDevitt, T.C. Pre-conditioning mesenchymal stromal cell spheroids for immunomodulatory paracrine factor secretion. *Cytotherapy* **16**, 331, 2014.
 46. Gonsalvez, D.G., Yoo, S.W., Fletcher, J.L., *et al.* Imaging and quantification of myelin integrity after injury with spectral confocal reflectance microscopy. *Front Mol Neurosci* **12**, 275, 2019.
 47. Brattain, K. *Analysis of the Peripheral Nerve Repair Market in the United States*. Minneapolis, MN: Magellan Medical Technology Consultants, Inc., 2014.
 48. Evans, G.R. Peripheral nerve injury: a review and approach to tissue engineered constructs. *Anat Rec* **263**, 396, 2001.
 49. Siemionow, M., and Brzezicki, G. Current techniques and concepts in peripheral nerve repair. *Int Rev Neurobiol* **87**, 141, 2009.
 50. Chomiak, T., and Hu, B. What is the optimal value of the g-ratio for myelinated fibers in the rat CNS? A theoretical approach. *PLoS One* **4**, e7754, 2009.
 51. Platz, J., Bonenfant, N.R., Uhl, F.E., *et al.* Comparative decellularization and recellularization of wild-type and alpha 1,3 galactosyltransferase knockout pig lungs: a model for ex vivo xenogeneic lung bioengineering and transplantation. *Tissue Eng Part C Methods* **22**, 725, 2016.
 52. Fang, J., Walters, A., Hara, H., *et al.* Anti-gal antibodies in alpha1,3-galactosyltransferase gene-knockout pigs. *Xenotransplantation* **19**, 305, 2012.
 53. Commins, S.P., James, H.R., Kelly, L.A., *et al.* The relevance of tick bites to the production of IgE antibodies to the mammalian oligosaccharide galactose- α -1, 3-galactose. *J Allergy Clin Immunol* **127**, 1286.e6, 2011.
 54. van Nunen, S. Tick-induced allergies: mammalian meat allergy, tick anaphylaxis and their significance. *Asia Pacific Allergy* **5**, 3, 2015.
 55. Van Nunen, S.A., O'Connor, K.S., Clarke, L.R., Boyle, R.X., and Fernando, S.L. An association between tick bite reactions and red meat allergy in humans. *Med J Aust* **190**, 510, 2009.
 56. Commins, S.P., Kelly, L.A., Rönmark, E., *et al.* Galactose- α -1, 3-galactose-specific IgE is associated with anaphylaxis but not asthma. *Am J Respir Crit Care Med* **185**, 723, 2012.

57. Commins, S.P., and Platts-Mills, T.A. Delayed anaphylaxis to red meat in patients with IgE specific for galactose alpha-1, 3-galactose (alpha-gal), *Curr Allergy Asthma Rep* **13**, 72, 2013.
58. Commins, S.P., Satinover, S.M., Hosen, J., *et al.* Delayed anaphylaxis, angioedema, or urticaria after consumption of red meat in patients with IgE antibodies specific for galactose- α -1, 3-galactose. *J Allergy Clin Immunol* **123**, 426.e2, 2009.
59. Platts-Mills, T.A., Schuyler, A.J., Hoyt, A.E., and Commins, S.P. Delayed anaphylaxis involving IgE to galactose-alpha-1, 3-galactose. *Curr Allergy Asthma Rep* **15**, 12, 2015.
60. Platts-Mills, T.A., Schuyler, A.J., Tripathi, A., and Commins, S.P. Anaphylaxis to the carbohydrate side chain alpha-gal. *Immunol Allergy Clin North Am* **35**, 247, 2015.
61. Wolver, S.E., Sun, D.R., Commins, S.P., and Schwartz, L.B. A peculiar cause of anaphylaxis: no more steak?. *J Gen Intern Med* **28**, 322, 2013.
62. Pattanaik, D., Lieberman, P., Lieberman, J., Pongdee, T., and Keene, A.T. The changing face of anaphylaxis in adults and adolescents. *Ann Allergy Asthma Immunol* **121**, 594, 2018.
63. Liang, R., Yang, G., Kim, K.E., *et al.* Positive effects of an extracellular matrix hydrogel on rat anterior cruciate ligament fibroblast proliferation and collagen mRNA expression. *J Orthop Transl* **3**, 114, 2015.
64. Fisher, M.B., Liang, R., Jung, H.J., *et al.* Potential of healing a transected anterior cruciate ligament with genetically modified extracellular matrix bioscaffolds in a goat model. *Knee Surg Sports Traumatol Arthrosc* **20**, 1357, 2012.
65. McGregor, C.G., Kogelberg, H., Vlasin, M., and Byrne, G.W. Gal-knockout bioprostheses exhibit less immune stimulation compared to standard biological heart valves. *J Heart Valve Dis* **22**, 383, 2013.
66. Liang, R., Fisher, M., Yang, G., Hall, C., and Woo, S.L. Alpha1,3-galactosyltransferase knockout does not alter the properties of porcine extracellular matrix bioscaffolds. *Acta Biomater* **7**, 1719, 2011.
67. McGregor, C., Byrne, G., Rahmani, B., Chisari, E., Kyriakopoulou, K., and Burriesci, G. Physical equivalency of wild type and galactose alpha 1,3 galactose free porcine pericardium; a new source material for bioprosthetic heart valves. *Acta Biomater* **41**, 204, 2016.
68. Huang, J.H., Cullen, D.K., Browne, K.D., *et al.* Long-term survival and integration of transplanted engineered nervous tissue constructs promotes peripheral nerve regeneration. *Tissue Eng Part A* **15**, 1677, 2009.
69. Wang, G., and Scott, S.A. The “waiting period” of sensory and motor axons in early chick hindlimb: its role in axon pathfinding and neuronal maturation. *J Neurosci* **20**, 5358, 2000.
70. Wang, L., and Marquardt, T. What axons tell each other: axon-axon signaling in nerve and circuit assembly. *Curr Opin Neurobiol* **23**, 974, 2013.

Address correspondence to:

D. Kacy Cullen, PhD

Center for Brain Injury & Repair

Department of Neurosurgery

Perelman School of Medicine

University of Pennsylvania

3320 Smith Walk, 105E Hayden Hall

Philadelphia, PA 19104

USA

E-mail: dkacy@pennmedicine.upenn.edu

Received: October 9, 2020

Accepted: January 11, 2021

Online Publication Date: April 8, 2021